Available online at www.sciencedirect.com
SCIENCE DIRECT®
PERGAMON
Polyhedron 22 (2003) 2331–2337
POLYHEDRON
www.elsevier.com/locate/poly

Ab initio calculations of the transfer parameters and coulombic repulsion and estimation of their effects on the electron delocalization and magnetic coupling in mixed-valence Keggin polyoxotungstates

Nicolas Suaud *, Alejandro Gaita-Ariño, Juan Modesto Clemente-Juan, José Sánchez-Marín, Eugenio Coronado

Instituto de Ciencia Molecular, Universidad de Valencia, C/Doctor Moliner 50, 46100 Burjassot, Spain

Received 7 October 2002; accepted 19 February 2003

Abstract

In this work, we present ab initio calculations on embedded fragments that permit to extract the value of the effective electron transfer integral and coulombic repulsion between W nearest neighbour atoms in a mixed-valence $\alpha PW_{12}O_{40}$ Keggin polyoxoanion. This allows us to perform a quantitative study of the influence of these two parameters on the magnetic properties of Keggin polyoxoanions reduced by two electrons. We surprisingly find that the electron transfer between edge-sharing and corner-sharing WO_6 octahedra have very close values, and show that the punctual charges estimation of coulombic repulsion may not be accurate enough to study the electronic distribution of the system. Finally, the parameters are introduced in a model Hamiltonian that represents the whole anion. The result is that electron transfers induce a large singlet–triplet gap in Keggin polyoxoanion reduced by two electrons, and so rationalizes its experimentally observed diamagnetism.

Keywords: Keggin anion; Electron transfer; Coulombic repulsion; Ab initio calculation; Magnetic coupling

1. Introduction

Polyoxometalates (POM) are discrete, anionic fragments of metal oxides, with a well-defined size and shape, ideally formed by fusion of regular polyhedra, specially tetrahedra, octahedra and square-based pyramids. POM are a rich and interesting class of inorganic compounds [1], showing attractive features for fields ranging from catalysis [2] to biomedicine [3] and including material science [4]. Additionally, they are good model systems for the study of magnetic and, more generally, electronic interactions. The possibility to control size, connectivity, angles and distances between the magnetic centers and the existence of families of structurally related compounds makes magnetostructural studies possible [5]. Their analogy to metal oxides and the fact that they are able to encapsulate magnetic transition metals and/or host delocalized 'blue' electrons [6,7] offers a vast field of interesting systems to study. Being much too complex to be fully treated by ab initio methods, they are usually studied by means of model Hamiltonians, which are extremely useful tools for predicting e.g. the magnetic properties of many systems.

Experimentally it is found that when reduced POM contain an even number of delocalized electrons, their spins are always completely paired, even at room temperature. This result is general and is observed not only in the Keggin structure subject of the present study, but also in other POM. It was initially attributed to a very strong antiferromagnetic coupling via a multiroute superexchange mechanism [8], but more recently it was theoretically shown that a combination of electron repulsion and electron delocalization can also stabilize the singlet ground state [9–11].

An extended-Hubbard model Hamiltonian adapted to reproduce the magnetic behaviour of a reduced Keggin anion encapsulating a diamagnetic ion should handle

* Corresponding author.
E-mail addresses: nicolas.suaud@uv.es (N. Suaud), eugenio.coronado@uv.es (E. Coronado).

0277-5387/03/$ - see front matter
doi:10.1016/S0277-5387(03)00307-3

with the following effective parameters corresponding to the main microscopic interactions:

- the t_1 electron transfer (hopping) parameter between edge-sharing octahedra,
- the t_2 electron transfer (hopping) parameter between corner-sharing MO_6 octahedra,
- the U on-site electron repulsion between electrons belonging to the magnetic orbital of a same metal center,
- the five $V_1 \ldots V_5$ inter-site electron repulsions corresponding to the five inequivalent pairs of metal centers, V_1 being the repulsion between nearest magnetic centers, V_2 the repulsion between next-nearest magnetic centers... V_5 the repulsion between farthest magnetic centers.

This model provides the relative energies of the different spin states and thus permits to predict the magnetic properties arising from any set of parameters. Several possible scenarii may be constructed, assuming certain parameter ratios. Unfortunately, the space spanned by this number of parameters is too large to permit an univocal solution of the problem. A realistic prediction of the magnetic properties of the compound under study needs the introduction in the model of realistic values of the parameters. Many experimental sources of information are available (susceptibility or calorimetric data, Electronic Paramagnetic Resonance or Inelastic Neutron Scattering experiments) but the physics governing the electronic interactions is often so complex that an extraction of the value of the parameters of the model Hamiltonian cannot (always) be obtained from these experiments. In order to reduce the size of the space spanned by the model Hamiltonian and to draw a picture of the coupling between the two delocalized electrons, independent informations on the values of these parameters are essential.

The aim of the present article is precisely to shine some theoretical light onto some of these parameters. We use very accurate ab initio methods to calculate the transfer parameters for the three closest neighbours in the Keggin structure. We also present some preliminary evaluations of the coulombic repulsion parameters using the same methods. The calculated values are then introduced in a model Hamiltonian based on the extended Hubbard model so that to obtain information about the low lying spin levels of the system, to calculate the effective coupling between the pair of delocalized 'blue' electrons and to rationalize the experimental magnetic properties of the system.

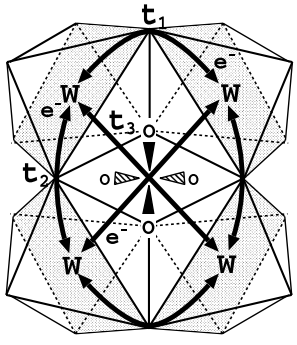

Fig. 1. The PW_4O_{20} fragment. The oxygen atoms occupy the corners of the octahedra or pyramids. The atoms modeled by punctual charges and TIP are not represented.

2. Methodology

Embedded fragment spectroscopy calculations focus on the 'fragment' of the system on which the studied process takes place (in our case the electron transfer or the coulombic repulsion). The fragment is treated by ab initio methods whereas the effects of the rest of the crystal (short-range Pauli exclusion and long-range Madelung potential) are reproduced by the mean of an embedding. The relativistic effects are taken into account in the formation of the set of orbitals used in this work. Indeed, a core models the effect of the inner electrons ($[1s^2 2s^2 2p^6 3s^2 3p^6 4s^2 3d^{10} 4p^6 5s^2 4d^{10} 4f^{14}]$ for the W atoms and $[1s^2]$ for the O and P atoms [12]) whereas large basis sets are used to treat the other electrons. The embedding consists in a large number of punctual charges and total-ion pseudopotentials (TIP) [13]: (i) a quasi-spherical bath of punctual charges is obtained by replacing all the atoms surrounding the fragment (those closer than 20 Å from the center of the considered Keggin anion) by punctual charges: (ii) TIP are put in the position of all the atoms of the first and second shells enclosing the fragment. In Refs. [14–16] a complete description of embedded fragment spectroscopy calculations is reported as well as a discussion of the accuracy of the embedding procedure.

The transfer (hopping) effective integrals are essentially local parameters [17], i.e. they describe a local phenomenon that is not significantly affected by dynamical processes involving other atoms than the two metal centers (between which the two electrons jump) or the oxygen ions of their coordination sphere [16]. Therefore, embedded fragment spectroscopy calculations can be used to accurately evaluate their values.

In order to cross-check the consistency and validity of our results, we consider several possible fragments for our calculations, namely

- a PW_4O_{20} tetranuclear fragment (Fig. 1) from which we can extract simultaneously all relevant parameters in our study,
- a W_4O_{16} tetranuclear fragment (Fig. 2), to check the influence of the PO_4 unit,

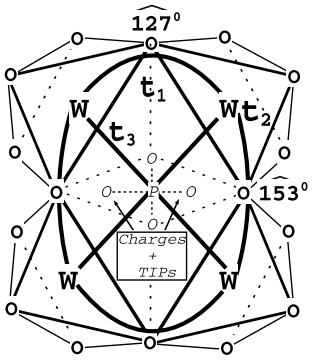

Fig. 2. The W_4O_{16} fragment. The atoms of the PO_4 clathrate modeled by punctual charges and TIP are represented whereas the other atoms modeled by punctual charges and TIP are not represented.

- two independent W_2O_9 dinuclear fragments and a W_2O_{10} dinuclear fragment (Figs. 3–5), contained in the tetranuclear fragments, in order to get alternative and independent estimations of the parameters and so allow a checking of the accuracy of the calculations.

For computational reasons, it is highly favourable to deal with a very symmetric structure. Therefore, our calculations are based on the X-ray crystallographical coordinates [18] of the $(H_5O_2^+)_3(PW_{12}O_{40}^{3-})$ salt, which has T_d symmetry making all the W atoms equivalent. On the one hand this high symmetry permits much quicker calculations. On the other hand, the equivalence of all the W ions induces the equivalence of all the interactions along edge-sharing octahedra as well as all the interactions along corner-sharing octahedra and of all interactions between second neighbour octahedra.

As a further cross-checking, the calculations are done at three different levels, with the Complete Active Space Self Consistent Field (CASSCF) method, with the second order multiconfigurational perturbation theory (CASPT2) [19] method and with the Difference Dedicated Configuration Interaction (DDCI) [20,21] method. CASSCF exactly treats the interactions between the magnetic electrons in the mean field of the remaining electrons, while CASPT2 adds a perturbative evaluation of the main effects lacking at the CASSCF level. DDCI is often considered as a reference in such kind of studies. It treats variationally the main dynamical effects that contribute to the phenomena under consideration. The use of different levels of calculation is of great help in order to confirm the consistency of the study. Indeed, CASPT2 and DDCI calculations include the main dynamical effects using the CASSCF results as a zeroth order and permit to check that the CASSCF takes into account the main physical effects governing the amplitude of the electron transfer, magnetic coupling or electronic repulsion.

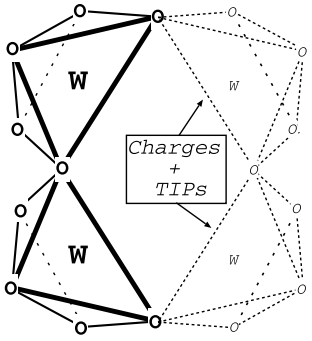

Fig. 3. The 2W-based fragment for the corner-sharing octahedra. The atoms that belong to the W_4O_{16} fragment but not to the present dimeric fragment are represented whereas the other atoms modeled by punctual charges and TIP are not represented.

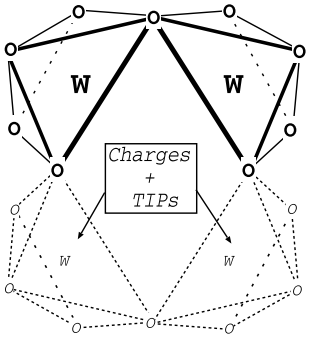

Fig. 4. The 2W-based fragment model for the edge-sharing octahedra. The atoms that belong to the W_4O_{16} fragment but not to the present dimeric fragment are represented whereas the other atoms modeled by punctual charges and TIP are not represented.

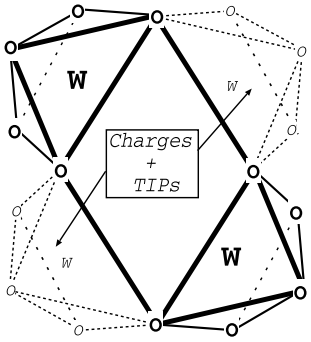

Fig. 5. The 2W-based fragment model for the next-nearest neighbour octahedra. The atoms that belong to the W_4O_{16} fragment but not to the present dimeric fragment are represented whereas the other atoms modeled by punctual charges and TIP are not represented.

3. Results and discussion

3.1. Calculations of electron transfers on tetrameric fragments

CASSCF and CASPT2 calculations are performed on both 4W-based fragments. The results are summarized in Table 1. We surprisingly find that t_1 and t_2 have very

similar values. This seems to be against usual magnetostructural correlations that would predict a high t_2/t_1 ratio. Indeed, the W–O–W angle between the two W ions and the bridging oxygen (that governs the overlap between the magnetic orbitals and the p-orbitals of this oxo anion) are very different. While for edge-sharing octahedra this angle is 127°, for corner-sharing octahedra it is 153°. A checking of the magnetostructural correlations is presented in the Section 3.3. The study also yields a non-zero value for t_3, which is usually neglected. It was found to be about four times smaller than t_1 and t_2, and of the same sign.

As a final result of this section, the very small differences between the results extracted on the PW_4O_{20} and W_4O_{16} fragments point towards an important conclusion: the PO_4^{3-} anion can magnetically be considered as a clathrate encapsulated in a neutral $W_{12}O_{36}$ cage, as already proposed in Ref. [22]. Indeed, the bridging effects due to the O anions of the PO_4 molecule are very small, as it could have been expected due to the large distance ($\simeq 2.5$ Å) between these anions and the W atoms (note that the electron transfer pathways from one W atom to the other through the PO_4 molecule are allowed in the PW_4O_{20} fragment but not in the W_4O_{16} fragment). The effects of the atoms of the PO_4 molecule on the transfer integrals are basically electrostatic average effects, they do not provide any electron transfer pathway. In the next section we show how calculations on dimeric fragments permit both to check the consistency of the method and to get more accurate and reliable parameters.

3.2. Calculations of electron transfers on dimeric fragments

Parameters t_1, t_2 and t_3 are extracted from 2W-based fragments. The results are included in Table 1. In contrast with calculations on tetramers, the extraction of parameters from calculations on dimers is direct: each transfer parameter is related to a single and independent energy difference. Despite this, we can see that the values extracted from the t_1 and t_2 parameters are very similar, confirming that the dimeric fragment can be considered a quite good model to evaluate these two transfer parameters in a more efficient and simple way. This is not the case with t_3. We can see that the values extracted from calculations on dimers and those extracted from 4W-based fragments differ significantly. This was up to some point theoretically unsurprising. Whereas in all the other fragments all the closest neighbours of the oxo bridges are in the fragment, the environment of the oxo bridge in this case is not so accurately treated, part of their first neighbours being modeled by TIP (see Fig. 5). Nevertheless, the calculations on dimers do prove that the t_3 parameter has a non-negligible value and justify our choice to take this parameter into account in the model Hamiltonian.

Table 1
Result in milli electron volt of the calculations of the electron transfer parameters on the different tetrameric and dimeric fragments

	meV	PW_4O_{20}	W_4O_{16}	Dimers
t_1	CASSCF	−551	−551	−560
	CASPT2	−470	−479	−490
t_2	CASSCF	−506	−510	−510
	CASPT2	−428	−443	−445
t_3	CASSCF	−87	−89	−80
	CASPT2	−123	−125	−102

3.3. Check for magnetostructural correlations between W–O–W angle and electron transfer parameter

From magnetostructural arguments one can expect a dramatic influence of the bridging angle on the transfer parameter, as the former is supposed to govern the orbital overlap which determines the latter. Our results seem to disagree with these ideas, because we find t_1 to be similar to t_2, while the bridging angle in corner- and edge-sharing octahedra are very different. We planned a series of calculations in order to get a better understanding of the magnetostructural relations of the system.

We use 2W-based fragments to study the variation of the values of t_1 and t_2 with the W–O–W angle. We performed calculations on model fragments obtained by rotating each of the WO_5 pyramids around the bridging O atoms in the plane containing these atoms and the two W atoms. 20 model fragments were formed (10 for the transfer between edge-sharing octahedra and 10 for the transfer between corner-sharing octahedra) corresponding to variations of the W–O–W angles of -5 to $+5°$ around the real angles given by the X-ray structure (152.4° for corner-sharing WO_6 octahedra and 126.8° for edge-sharing octahedra). We did not perform calculations on more distorted fragments as they should be too far from the real structure to give relevant values.

According to our calculations, the transfer parameters increase in absolute value when the W–O–W angle increases. This is due to the increase of the overlap between the magnetic orbital of the W ions and the bridging orbital of the O ion. Such a variation is of the same order of magnitude for corner and edge-sharing fragments with a tangent at 152.4° of about −4.6 meV per degree and of about −3.9 meV per degree at 126.8° (at the CASPT2 level). If the W–O–W angle were the only geometrical parameter acting on the transfer parameter, this would mean that, always at CASPT2 level, at 152.4° (t_2) the transfer should be more than 100 meV more negative than at 126.8° (t_1), in contradiction with the tendencies exhibited in Table 1. Thus, we can conclude that other structural parameters than the W–

O–W angle strongly affect the electron transfer and should be taken into account both to explain why the values of t_1 and t_2 are close and when evaluating the electron transfer parameters in analogous systems.

3.4. Extraction of most accurate results of electron transfer parameters

The 2W-based fragments permit to perform a variational treatment of the dynamical effects on the transfer parameters using the DDCI method. This yields the following results, which are the most accurate ones presented in this work:

$t_1 = -507$ meV $\quad t_2 = -467$ meV

These values are in good agreement with those obtained at the CASSCF and CASPT2 level of calculations on the same fragments and on the 4W-based fragments. It confirms that t_1 and t_2 have almost equal intensities of about half an milli electron volt.

We do not perform analogous calculations to extract the t_3 parameter because the 'diagonal' dimer is not well suited for accurate calculations.

3.5. Calculation of the electronic repulsion

An evaluation of the electrostatic repulsion of the system considering punctual charges gives:

$V_1 \simeq 4100$ meV $\quad V_2 \simeq 3800$ meV $\quad V_3 \simeq 2800$ meV

that is:

$V_1 - V_3 \simeq 1300$ meV $\quad V_2 - V_3 \simeq 1000$ meV

To check the validity of these estimations, ab initio calculations were performed to extract the values of the electronic repulsion. Due to the nature of the fragments used in this paper, only the differences $V_1 - V_3$ and $V_2 - V_3$ can be determined. CASSCF calculations yield:

$V_1 - V_3 \simeq 1400$ meV $\quad V_2 - V_3 \simeq 1200$ meV

These results are in quite good agreement with point charge calculations. However, preliminary calculations at the CASPT2 level show important changes in the energy level spectrum that could induce a strong lowering of these values. Methodological incompatibilities between the procedure of extraction of the values and the CASPT2 method do not permit an accurate enough evaluation of the parameters at this level of calculation. Nevertheless, a rough estimation gives $V_1 - V_3 \simeq V_2 - V_3 \simeq 700$ meV.

As a conclusion, the real value of the electron repulsion in Keggin POM seems to be far from the over-simplistic evaluation considering punctual charges. An accurate DDCI calculation of the dynamical effects on the electron repulsions would require greater computational resources and will be the aim of a forthcoming paper.

3.6. Model Hamiltonians and magnetic properties

By the use of model Hamiltonians, previous works [10] have developed several possible scenarii for two-electron-reduced Keggin anion with different ratios between electron repulsion and electron transfer parameters, which lead to completely different magnetic behaviours. Fig. 6 represents the variation with the t_1/t_2 ratio of the energy levels assuming that the electrons remain on the two farthest magnetic centers, i.e. that the energy gaps $V_3 - V_4$ and $V_3 - V_5$ are larger than the electron transfer integrals. The vertical dashed line corresponds to the values of the transfer parameters obtained from ab initio calculations. Using these results the model Hamiltonian predicts a singlet 'diamagnetic' ground state and that the first excited state is a triplet state. The energy gap between these states is about 0.6 t_2, that is 280 meV, in clear agreement with the diamagnetic properties of two-electron-reduced Keggin anion compounds [8].

The results of further refinements are displayed in Fig. 7. It represents the evolution of the singlet–triplet energy gap with the ratio $V_3 - V_5/V_4 - V_5$. A infinite value of this ratio corresponds to the previous assumption, i.e. that the electrons remain on the two farthest centers. From this limit to an equality between V_3 and V_4 ($V_3 - V_5/V_4 - V_5 = 1$) the singlet to triplet energy gap monotonously increases from about $0.65 \times (V_4 - V_5)$ to $0.9 \times (V_4 - V_5)$. Taking into account into the model Hamiltonian the situations were the electrons are in next–next–nearest position thus results in an increase of the singlet–triplet energy gap and thus predicts a stronger diamagnetic behaviour of the compound.

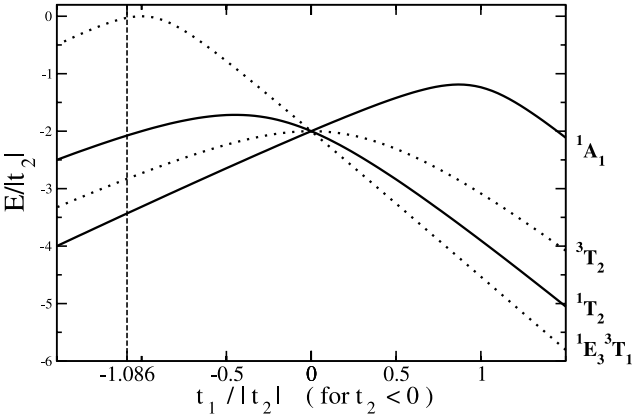

Fig. 6. Theoretical energy levels of the doubly reduced Keggin ion. The dotted lines stands for triplet states, the solid lines for singlet states (see Ref. [10] for the denomination of the states). The vertical dashed line representes the value of the calculated $t_1/|t_2|$ ratio.

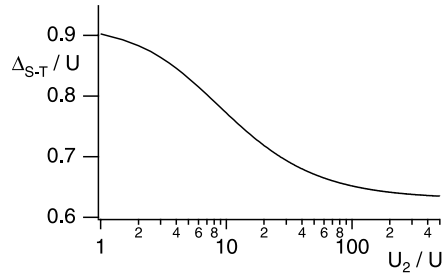

Fig. 7. Variation of the spin-triplet energy gap (in V_4-V_5 units) with the ratio $U_2/U = V_3-V_5/V_4-V_5$ for $t_2 = t_1 = -1$. Former assumptions correspond to the 'right side', new data point towards the 'left side'.

4. Conclusion

In this work, we show the efficiency of the combination of embedded fragment ab initio calculations with a model Hamiltonian approach to rationalize the magnetic behaviour of reduced POM. First, from comparisons between the results obtained on fragments of various nuclearities we check the accuracy of ab initio calculations to evaluate the amplitude of the electron transfer between W centers. We show that embedded fragments based on two corner-sharing WO_5 pyramids are large enough not to lack any important dynamical effect and small enough to permit their accurate variational treatment with the DDCI method. These fragments are used in a magnetostructural study that demonstrates that the W–O–W angle between the tungsten atoms and the bridging oxygen ions is not the only parameter governing the electron transfer. Then, the values of the transfer parameters are introduced in an extended-Hubbard model Hamiltonian suited to represent the magnetic behaviour of a two electron-reduced Keggin polyoxotungstate. Ab initio calculations of the electronic repulsion differ significantly from point charges estimations. These early estimations had justified some restrictions that had simplified the resolution of the model Hamiltonian. Even if the differences between ab initio and point charge calculations are large enough to encourage us to revise these conclusions, we show that the release of the restrictions will result in an enforcement of the predicted singlet–triplet energy gap of the system.

In conclusion, the combination of electron transfer and electronic repulsion is proven to be the origin of the strong diamagnetism of POM reduced by an even number of electrons.

Acknowledgements

This research was financially supported by European Community (Network Molnanomag, no. HPRN-CT-1999-00012), by the spanish Ministerio de Ciencia y Technología (MAT2001-3507) and by the Generalitat Valenciana (GV01-312). A.G.A. thanks the Generalitat Valenciana for a predoctoral grant. J.M.C.J. thanks the spanish Ministerio de Ciencia y Tecnología for a 'Ramón y Cajal' contract. We thank Marie-Bernadette Lepetit for many fruitful discussions.

References

[1] L. Hill (Ed.), Polyoxometalates, Chem. Rev. 98 (1998).
[2] (a) I.V. Kozhevnikov, Chem. Rev. 98 (1998) 171;
(b) N. Mizuno, M. Misono, Chem. Rev. 98 (1998) 199;
(c) M. Sadakane, E. Steckhan, Chem. Rev. 98 (1998) 219.
[3] J.T. Rhule, C.L. Hill, D.A. Judd, R.F. Schinazi, Chem. Rev. 98 (1998) 327.
[4] (a) A. Müller, F. Peters, M.T. Pope, D. Gatteschi, Chem. Rev. 98 (1998) 239;
(b) E. Coronado, C.J. Gómez-García, Chem. Rev. 98 (1998) 273;
(c) W.G. Klemperer, C.G. Wall, Chem. Rev. 98 (1998) 297;
(d) M.T. Pope, A. Müller, Polyoxometalates: From Platonic Solids to Anti-Retroviral Activity, Kluwer Academic Publishers, Dordrecht, The Netherlands, 1994.
[5] (a) J.M. Clemente-Juan, E. Coronado, Coord. Chem. Rev. 193–195 (1999) 193;
(b) J.M. Clemente-Juan, E. Coronado, Coord. Chem. Rev. 193–195 (1999) 361.
[6] N. Casañ-Pastor, P. Gomez-Romero, G.B. Jameson, L.C.W. Baker, J. Am. Chem. Soc. 113 (1991) 5658.
[7] M.T. Pope, Isopoly and Heteropoly Metalates, Springer, Berlin, 1983.
[8] (a) M. Kozik, C.F. Hammer, L.C.W. Baker, J. Am. Chem. Soc. 108 (1986) 2748;
(b) M. Kozik, L.C.W. Baker, J. Am. Chem. Soc. 109 (1987) 3159;
(c) M. Kozik, N. Casañ-Pastor, C.F. Hammer, L.C.W. Baker, J. Am. Chem. Soc. 110 (1988) 1697;
(d) M. Kozik, L.C.W. Baker, J. Am. Chem. Soc. 112 (1990) 7604;
(e) N. Casañ-Pastor, L.C.W. Baker, J. Am. Chem. Soc. 114 (1992) 10384.
[9] (a) S.A. Borshch, B. Bigot, Chem. Phys. Lett. 212 (1993) 398;
(b) H. Duclusaud, S.A. Borshch, J. Am. Chem. Soc. 123 (2001) 2825.
[10] J.J. Borrás-Almenar, J.M. Clemente-Juan, E. Coronado, B.S. Tsukerblat, Chem. Phys. 195 (1995) 1.
[11] (a) J.J. Borrás-Almenar, J.M. Clemente-Juan, E. Coronado, B.S. Tsukerblat, Chem. Phys. 195 (1995) 17;
(b) J.J. Borrás-Almenar, J.M. Clemente-Juan, E. Coronado, B.S. Tsukerblat, Chem. Phys. 195 (1995) 29.
[12] Z. Barandiarán, L. Seijo, Can. J. Chem. 70 (1992) 409.
[13] P. Durand, J.C. Barthelat, Theor. Chim. Acta 38 (1975) 283.
[14] (a) C. Jimenez Calzado, J. Fernandez Sanz, J.P. Malrieu, F. Illas, Chem. Phys. Lett. 307 (1999) 102;
(b) D. Munoz, F. Illas, I. de P.R. Moreira, Phys. Rev. Lett. 84 (2000) 1579;
(c) C. Jimenez Calzado, J. Fernandez Sanz, J.P. Malrieu, J. Chem. Phys. 112 (2000) 5158.
[15] (a) N. Suaud, M.-B. Lepetit, Phys. Rev. B 62 (2000) 402;
(b) N. Suaud, M.-B. Lepetit, Phys. Rev. Lett. 88 (2002) 056405.
[16] M.-B. Lepetit, N. Suaud, A. Gelle, V. Robert, J. Chem. Phys. 118 (2003) 3966.
[17] I. de P.R. Moreira, F. Illas, C.J. Calzado, J.F. Sanz, J.P. Malrieu, N. Ben Amor, D. Maynau, Phys. Rev. B 59 (1999) 6593.
[18] G.M. Brown, M.-R. Noe-Spirlet, W.R. Busing, H.A. Levy, Acta Crystallogr. B 33 (1977) 1038.
[19] MOLCAS Version 5.2 K. Andersson, M. Barysz, A. Bernhardsson, M.R.A. Blomberg, Y. Carissan, D.L. Cooper, M. Cossi, T. Fleig,

M.P. Fülscher, L. Gagliardi, C. de Graaf, B.A. Hess, G. Karlström, R. Lindh, P.-Å. Malmqvist, P. Neogrády, J. Olsen, B.O. Roos, B. Schimmelpfennig, M. Schütz, L. Seijo, L. Serrano-Andrés, P.E.M. Siegbahn, J. Stålring, T. Thorsteinsson, V. Veryazov, M. Wierzbowska, P.-O. Widmark, Lund University, Sweden, 2001.

[20] (a) J.P. Malrieu, J. Chem. Phys. 47 (1967) 4555;
(b) R. Broer, W.J.A. Maaskant, Chem. Phys. 102 (1986) 103;
(c) J. Miralles, O. Castell, R. Caballol, J.P. Malrieu, Chem. Phys. 172 (1993) 33;
(d) J. Cabrero, N. Ben Amor, C. de Graaf, F. Illas, R. Caballol, J. Phys. Chem. A 104 (2000) 9983.

[21] (a) CASDI suite of programs. D. Maynau, N. Ben Amor, J.V. Pitarch-Ruiz, University of Toulouse, France, 1999.;
(b) N. Ben Amor, D. Maynau, Chem. Phys. Lett. 286 (1998) 211;
(c) J.V. Pitarch-Ruiz, J. Sánchez-Marín, D. Maynau, J. Comp. Chem. 23 (2002) 1157.

[22] (a) C. Rocchiccioli-Deltcheff, R. Thouvenot, R. Franck, Spectrochim. Acta 32A (1976) 587;
(b) R. Acerete, N. Casañ-Pastor, J. Bas-Serra, L.C.W. Baker, J. Am. Chem. Soc. 111 (1989) 6049;
(c) L.P. Kazansky, B.R. McGarvey, Coord. Chem. Rev. 188 (1999) 157;
(d) J.M. Maestre, X. Lopez, C. Bo, J.-M. Poblet, N. Casañ-Pastor, J. Am. Chem. Soc. 123 (2001) 3749;
(e) X. López, J.M. Maestre, C. Bo, J.-M. Poblet, J. Am. Chem. Soc. 123 (2001) 9571.